JOURNAL OF APPLIED PHYSICS VOLUME 91, NUMBER 5 1 MARCH 2002

# Correlation between photoluminescence properties and morphology of laser-ablated Si/SiO$_x$ nanostructured films

A. V. Kabashin,[a] J.-P. Sylvestre, S. Patskovsky, and M. Meunier
*Ecole Polytechnique de Montréal, Département de Génie Physique et Groupe de recherche en physique et technologie des couches minces (GCM), Case Postale 6079, succ. Centre-ville, Montréal (Québec), Canada, H3C 3A7*

(Received 13 February 2001; accepted for publication 27 November 2001)

Pulsed laser ablation in an inert gas has been used to fabricate films containing silicon nanocrystals. We show that film microstructure is one of the main factors, determining long-term photoluminescence (PL) properties. Films with different porosity were found to exhibit PL signals with quite different peak energies, integral intensities and time-dependent evolutions. The distinction of these PL properties is attributed to the different efficiency of surface chemistry interactions between Si nanocrystallites and the ambient atmosphere for films having different porosities. Oxygen-related defects and other mechanisms are discussed to explain the PL properties of the films. © *2002 American Institute of Physics.* [DOI: 10.1063/1.1446217]

## I. INTRODUCTION

Significant effort has been focused in recent years on the fabrication and characterization of Si-based nanocrystallites (see, e.g., Refs. 1–10). These nanostructured materials can exhibit visible photoluminescence (PL) with quantum efficiency of up to few percent, although crystalline silicon has a small (1.11 eV at room temperature) and indirect band gap. This property gives a promise for the creation of silicon-based optoelectronics devices and their integration in standard silicon technology. ''Dry'' fabrication techniques, such as pulsed laser ablation (PLA), are of particular interest for these applications due to their good compatibility with silicon processing technology.

Nevertheless, the origin and properties of PL are still under debate. The appearance of PL was usually connected to the presence of nanoscale crystallites in the deposit, while different mechanisms such as quantum confinement effect,[1] surface radiation states,[2] defects in $SiO_2$ structure[3] etc. were proposed to explain PL characteristics. The difficulty of a clear identification of PL mechanisms is mainly due to quite different PL properties reported by different groups. Some groups reported nearly similar peaks for various grain sizes (see, e.g., Refs. 2, and 4–7), whereas other teams observed a clear shift of PL peak when the particle size was changed by a variation of deposition conditions as follows from quantum confinement model (see, e.g., Refs. 8 and 9). In our opinion, many aspects of the phenomenon could be clarified if one considers a correlation of PL properties not only with the grain size, but with film morphology and chemical composition as well.

PLA is known as one of the most flexible techniques for fine variation and control of nanocluster parameters during the deposition.[11–13] In this article, we used PLA methods for a preparation of Si-based films with different nano- and microstructure and examine the correlation of these parameters with PL characteristics.

[a]Electronic mail: akabach@email.phys.polymtl.ca

## II. EXPERIMENTAL SETUP

Radiation of a pulsed KrF laser [$\lambda=248$ nm, pulse length—15 ns full width at half maximum and repetition rate 30 Hz] was used for the ablation of material from a rotating Si target [(1-0-0), N-type, resistance 10 Ohm cm]. The radiation was focused on a focal spot $2\times1$ mm$^2$ on the target at the incident angle of 45° giving the radiation intensity of about $5\times10^8$ W/cm$^2$. The substrates, identical to the target, were placed on a rotating substrate holder at 2 cm from the target. The experimental chamber was pumped down to $P=2\times10^{-7}$ Torr before filling with helium (purity 99.9995%) for a deposition at a constant pressure $P$ ranging between 0.05 and 10 Torr. Under the residual air pressure of $2\times10^{-7}$ Torr and the laser repetition rate of 30 Hz, oxidation of ablated silicon layers is negligible between the laser pulses.[9] The film thickness after several thousands laser shots was 100–700 nm. In some cases, the films were annealed at 800 °C in air for 10 min. The increase and decrease rates were 10 °C/min.

The PL spectra were recorded on a double spectrometer (U100, Instruments SA) using 488-nm radiation of an $Ar^+$ laser with power density of 30 W/cm$^2$ as a source and a GaAs photomultiplier as the detector. Scanning electron microscopy (SEM), atomic force microscopy (AFM), x-ray diffraction (XRD), and specular x-ray reflectivity[14] (SXRR) spectroscopies were used to examine structural properties of the films. In addition, x-ray photoemission spectroscopy (XPS) was used to determine the surface layer composition.

## III. STRUCTURAL PROPERTIES

First of all, we examined the size of silicon particles produced by the pulsed laser deposition process. A fraction of a monolayer of clusters was deposited on a substrate of highly oriented pyrolitic graphite (HOPG), which is known to have an atomically flat surface. The size of the particles was recorded by the AFM technique in the ''tapping'' mode. A typical AFM image of several isolated laser-ablated particles is shown in Fig. 1(a), while Fig. 1(b) presents a two

0021-8979/2002/91(5)/3248/7/$19.00  © 2002 American Institute of Physics

Downloaded 25 Feb 2002 to 132.204.56.48. Redistribution subject to AIP license or copyright, see http://ojps.aip.org/japo/japcr.jsp

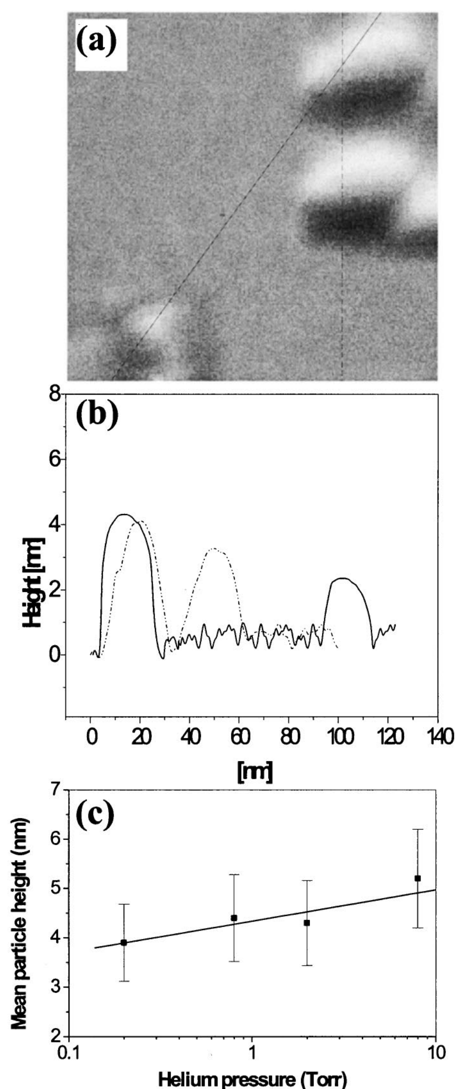


FIG. 1. (a) AFM image of isolated laser-ablated particles on graphite (HOPG) substrate, (b) Profile analysis of the AFM image over the solid and dashed lines, and (c) Mean particle height from AFM images as a function of helium pressure during the deposition.

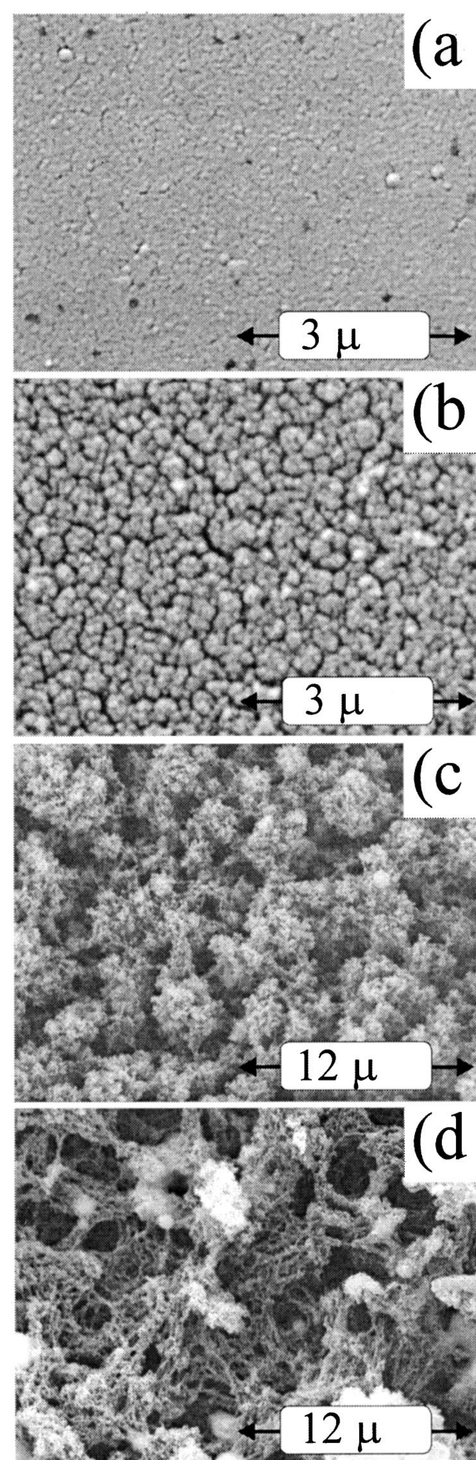


FIG. 2. SEM images of the laser-ablated films fabricated under 1 Torr (a), 2 Torr (b), 4 Torr (c), and 8 Torr (d).

profile analysis of the image. One can see that the height of the particles was about 2–4 nm, while their recorded lateral dimensions were about 20–30 nm. It is known that real size of nanoobjects is truly presented only by the height measurements, while their lateral dimensions are usually enlarged due to the tip–object convolution effect. Therefore, we may conclude that the real size of the smallest ablated particles was about 2–3 nm, which is in agreement with previous studies of laser-ablated Si-based deposits by transmission electron microscopy (4–10 nm)[5] and AFM (1–10 nm)[6,9,15] techniques. However, larger particles with dimensions of about 10–15 nm were also present in some images. Performing the depositions under different helium pressures, we were able to clarify the influence of the pressure on the mean nanoparticle size. As shown from Fig. 1(c), the mean size increased with helium pressure, though the size variations did not exceed 1 nm. This is also in good agreement with pressure dependence of mean nanocrystal size reported in previous studies.[6,9,15]

Continuous films formed by the multipulse deposition were colored. While deposited under pressures $P$ below 1–1.5 Torr, the films showed distinct multicolor interference fringes due to nonuniformity in the film thickness. However, for $P>1.5$ Torr, the fringes were absent and the films were yellow or yellow-gray deposits. The absence of fringes was

Downloaded 25 Feb 2002 to 132.204.56.48. Redistribution subject to AIP license or copyright, see http://ojps.aip.org/japo/japcr.jsp

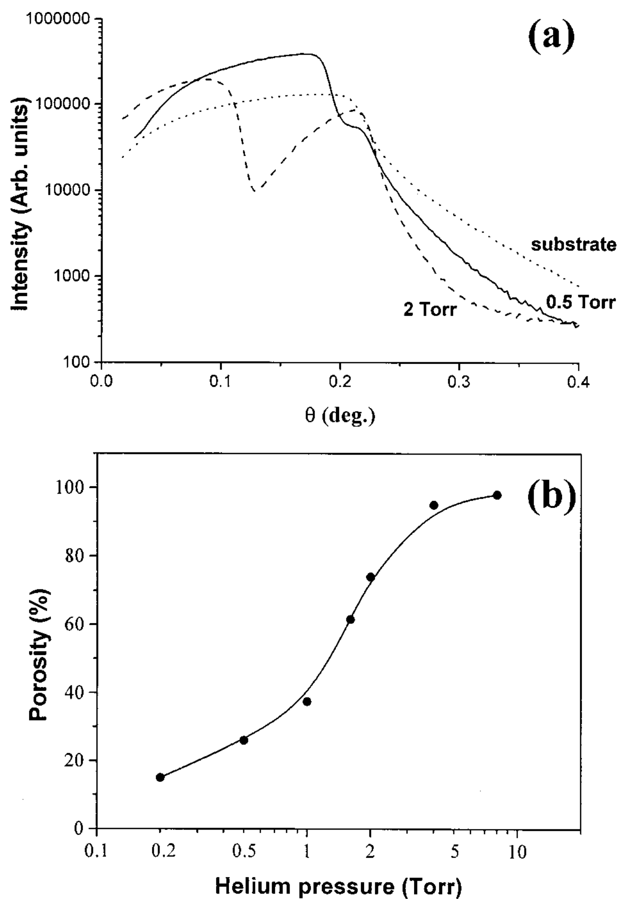


FIG. 3. (a) Typical SXRR curves for a silicon wafer (substrate) and laser-ablated films fabricated at 0.5 and 2 Torr of helium. (b) Porosity of the films estimated from SXRR curves as a function of helium pressure during the deposition.

probably because of a granular, porous-like microstructure of the deposit for high pressures, which prevented the interference in reflected white light. As shown in Fig. 2, SEM studies of film morphology confirmed the assumption that the porosity increases gradually with the increase of the helium pressure. While only initial signs of roughness were discerned with the films deposited under 1 Torr, the experiment under 2 Torr provided a developed porous structure with pore size of about 50–100 nm. Further pressure increase up to 4 Torr led to a formation of web-like aggregations of particles. Note that under $P<1$ Torr, the roughness details were too small to be detected by our SEM system. Thus, our experiments clearly show that not only the mean particle size, but also the morphology of the films is sensitive to the deposition conditions.

To characterize quantitatively the porosity of the laser-ablated films, we applied a technique of SXRR.[14] SXRR spectra were obtained with the use of a simple powder x-ray diffractometer, which made possible a monitoring of the intensity of an x-ray beam reflected from a surface under a simultaneous $\theta$–$2\theta$ scanning of a source and a detector ($0° < \theta < 1°$, $\theta$ was measured towards the surface). Since for x-rays, the refractive index of most materials is less than 1, a phenomenon of total external reflection occurs for $\theta < \theta_c$, while for $\theta > \theta_c$, the reflected intensity suffers a rapid attenuation. Because $\theta_c$ is proportional to the square root of the electronic density, which is directly proportional to the density of the material, the experimental determination of the critical angle gives access to the density of the material.[14,16,17] For a given material, a porosity increase results in the density decrease, which can be quantified by a decrease of the critical angle:

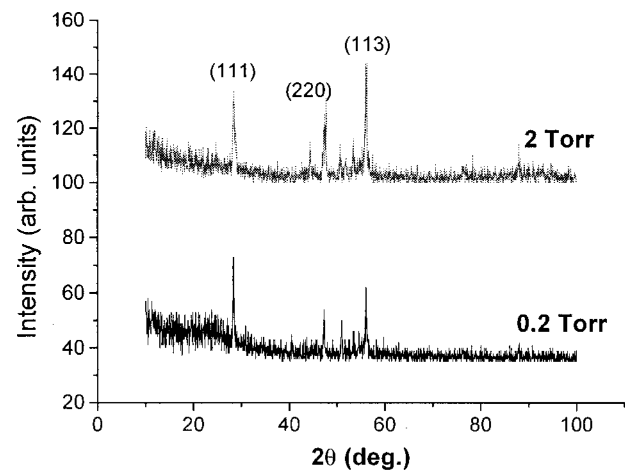


FIG. 4. Typical x-ray diffraction spectra from laser-ablated films fabricated at 0.2 and 2 Torr of helium.

$$\text{porosity}(\%) = 100\left(1 - \frac{\theta_c^2}{\theta_{c\ \text{bulk Si}}^2}\right), \tag{1}$$

where $\theta_c$ and $\theta_{c\ \text{bulk Si}}$ are the critical angles from SXRR spectra for a thin film and bulk silicon, respectively.

Experimental reflectivity curves for a silicon substrate (wafer) with and without laser-ablated films are presented in Fig. 3(a). One can see that the critical angle for the substrate $\theta_{c\ \text{bulk Si}}$ was about 0.22°, which is in good agreement with previous studies.[18] Similar substrate-related angle of 0.22° could be observed for all samples with laser-ablated films as shown in Fig. 3(a). In addition, the later samples contained an additional air/film interface-related critical angle $\theta_c$, whose position depended on helium pressure. For example,

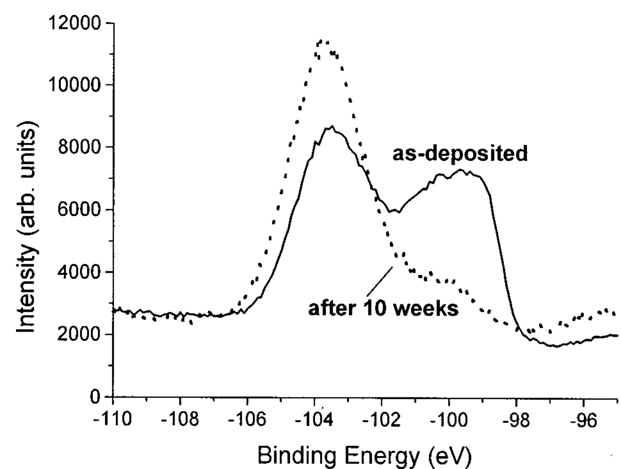


FIG. 5. Typical XPS spectra from the films prepared by laser ablation just after their fabrication and after ten weeks of their exposition to ambient air.

Downloaded 25 Feb 2002 to 132.204.56.48. Redistribution subject to AIP license or copyright, see http://ojps.aip.org/japo/japcr.jsp

for the films deposited at 0.5 Torr and 2 Torr, we had $\theta_{c1}=0.19°$ and $\theta_{c2}=0.11°$, respectively [Fig. 3(a)]. Substituting the values of $\theta_{c1}$ and $\theta_{c2}$ into Eq. (1), we obtain the film porosities of 25% and 75%, respectively. Figure 3(b) summarizes the porosity measurements for laser-ablated films deposited under different pressures $P$. Here, a tendency of the porosity enhancement with the pressure increase is quite clear for $P<2$ Torr, while for higher pressures the porosity always exceeds 95%. It is necessary to note that the precision of SXRR measurements was about 10%.

An x-ray diffractometer was also used to examine the film crystallinity. As shown in Fig. 4, XRD spectra of the laser-ablated films exhibited all peaks typical for crystalline silicon. In addition, an analysis of XRD spectra of some samples deposited at reduced pressures $P=0.2-0.5$ Torr indicated the presence of a minor amorphous phase.

The surface composition of the films was examined by XPS. Figure 5 shows the XPS spectra of a film just after its fabrication (spectrum 1) and after eight weeks of its exposition to ambient air (spectrum 2). The spectrum of the as-deposited sample (1) demonstrates two peaks at about 99.8 and 103.2 eV, which are assigned to the Si 2$p$ photoelectrons of the unoxidized Si core and the $SiO_x$ oxide layer, respectively. The spectrum of the oxidized sample (2) reveals a decrease of the low-energy peak with a slight shift to higher binding energies. On the other hand, the high-energy peak becomes stronger and shifts to higher energies up to 104 eV, which is assigned to 2$p$ photoelectrons of pure $SiO_2$. Our XPS results shown in Fig. 5 agree well with those of previous studies of $SiO_x$ films (see, e.g., Ref. 19), suggesting that the composition $x$ of the surface oxide increases as the exposition time increases.

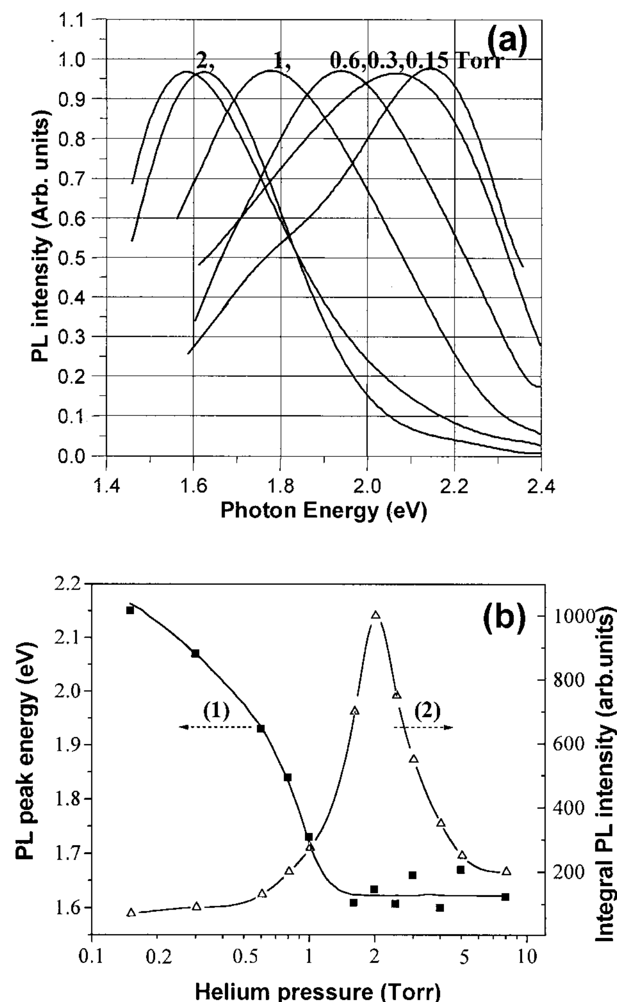


FIG. 6. (a) PL spectra of $Si/SiO_x$ films deposited at different He pressures. Spectra intensities are normalized to the peak value. (b) PL peak energy (1) and integral PL intensity (2) as a function of the helium pressure for as-deposited films.

## IV. PHOTOLUMINESCENCE PROPERTIES

Signals of visible PL were observed only after the exposition of the films to oxygen, i.e., after the replacement of helium in the experimental chamber by ambient air. The films deposited under different helium pressures showed quite different PL characteristics. For films deposited at reduced pressures $P<1.5$ Torr, we recorded PL spectra with peak energy position strongly depending on the pressure as shown in Fig. 6(a). The pressure dependencies for peak energy position and integral intensity of the PL signals are presented in Fig. 6(b). One can see that a pressure increase from 0.15 to 1.5 Torr in different depositions caused a redshift of the peak from 2.12 to 1.6–1.7 eV. However, for films deposited at relatively high pressures $P>1.5$ Torr, we observed quite different PL signals. The peak energy of these signals was always around 1.6–1.7 eV and did not depend on helium pressure during the deposition. In addition, the intensity of 1.6–1.7 eV signals was much stronger, while the most efficient PL was reported with the films deposited at 2 Torr [Fig. 6(b)].

Our experiments showed that oxidation phenomena could lead to a dramatic modification of PL properties from laser-ablated films. First of all, we observed a considerable enhancement of integral intensity of 1.6–1.7 eV signals under a prolonged storage of the films in pure dry air as shown in Fig. 7(a) (spectra 1–3). The intensity could increase by a factor of 4–10 and stabilized only after eight to twelve weeks, while the increase rate depended on the relative air humidity. The enhancement was accompanied by a slight redshift of the peak energy position as shown in Fig. 7(a). It is necessary to note that the 1.6–1.7 eV signals were recorded only with films deposited at relatively high helium pressures $P>1.5$ Torr. The common property of these films was relatively high porosity, which exceeded 40% [Fig. 3(b)]. Figure 7(b) presents the dependence of the integral intensity of the PL signals on film porosity. One can clearly see that only highly porous films demonstrated PL intensity enhancement. On the other hand, blueshifted PL signals from low porous films remained stable even after their prolonged storage in air.

Secondly, we observed an appearance of an additional PL peak at about 2.2–2.3 eV under a prolonged storage of porous samples (with porosity higher than 40%) in humid air environment (relative humidity 80%–100%), as shown in Fig. 7(a) (spectrum 4). Similar 2.2–2.3 eV component appeared after the thermal annealing of all as-deposited films (spectrum 5), regardless of their porosity. It is important to

Downloaded 25 Feb 2002 to 132.204.56.48. Redistribution subject to AIP license or copyright, see http://ojps.aip.org/japo/japcr.jsp

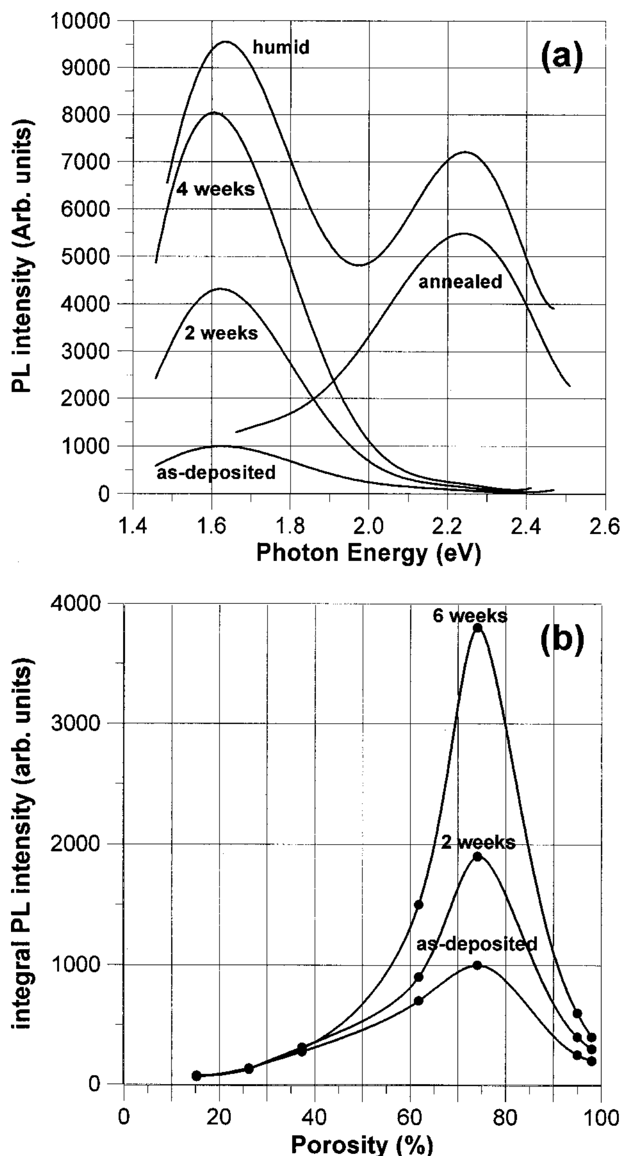


FIG. 7. (a) PL spectra from Si/$SiO_x$ films deposited by PLA under $P=2$ Torr: as-deposited, after two weeks and four weeks of film storage in dry air; after eight weeks of the of the storage in humid air (humid); and after the thermal annealing (annealed). (b) Integral intensity of PL signals as a function of film porosity under a prolonged storage of the films in dry air.

mention that the appearance and enhancement of 1.6–1.7 eV and 2.2–2.3 eV components correlated well with the relative increase of $x$ in oxygen-related $SiO_x$ complexes $(0<x<2)$ of the upper film layer, as measured by XPS (Fig. 5). This correlation between spectral and surface composition modifications gives evidence for oxidation-related origin of these components.

Nevertheless, the oxidation-related PL components showed quite different responses to photochemical or chemical modification of the films. In particular, the 2.2–2.3 eV component suffered a dramatic PL intensity degradation after a few minutes of continuous irradiation by $Ar^+$ laser radiation, while the 1.6–1.7 eV one remained almost stable even after 6 h of the illumination. In another test, a chemical attack of the films by a 10% solution of HF for 5 min led to almost complete vanishing of the PL intensity for the 2.2–2.3 eV component and much weaker three- to five-fold intensity decrease for the 1.6– 1.7 eV component. The intensity decrease for the latter component was accompanied by a "blueshift" of its peak energy from 1.6–1.65 to 1.75–1.8 eV. Nevertheless, several weeks of the film exposition to ambient air led to a complete recovery of both the intensity and peak position for the 1.6–1.7 eV component, while 2.2–2.3 eV signals remained weak. Such a different response to the photochemical and chemical modifications gives evidence for different mechanisms responsible for the two components.

## V. DISCUSSION

Our studies have clearly shown that ablation conditions are critical not only for the crystallite size in the deposit, but for the film microstructure as well. Even minor variations of the gas pressure during deposition cause a dramatic change of film porosity. We believe that this phenomenon is related to peculiarities of silicon nanocluster formation during the laser-ablation process. Collisions with light helium atoms cause a cooling of the clusters and their size enlargement. Under relatively low pressures, a number of collisions are not sufficient to condense and crystallize the clusters in gaseous phase. Therefore, the clusters in the gas phase are relatively hot and crystallize when they arrive on the substrate forming a dense and well-packed crystalline film, as one can see in Fig. 2(a). Under high pressures, more frequent collisions lead to a fast cooling and more effective condensation of clusters in the gaseous phase. As a result, they arrive on the substrate with larger size, being partially crystallized and having an arbitrary shape, which causes a formation of highly porous layers and even web-like agglomerations, as shown in Figs. 2(c) and 2(d).

We propose that it is the microstructure difference that causes the dramatic distinction of long-term PL properties for the films deposited at low and high pressures. Dense and self-coagulated structures of the films fabricated under $P<1$ Torr minimize the impact of ambient atmosphere on the film properties. Indeed, we did not detect any remarkable changes of PL spectra even after a prolonged natural oxidation of low porous films [Fig. 7(b)]. We believe that PL mechanisms related to core silicon crystals are predominant for these films, though the upper surface oxide can also play a certain role in a formation of PL centers. In particular, the redshift of the spectra under an increase of helium residual pressure could be due to the quantum confinement mechanism.[1] In this case, an air passivation of the nanoclustered film is necessary to saturate dangling bonds, thus reducing nonradiative recombination channels. This supposition is confirmed by the increase of mean particle height on AFM images with the increase of helium pressure [Fig. 1(c)]. Nevertheless, other mechanisms may not be ruled out completely.

The porosity enhances the surface area, which is subjected to surface chemistry modifications due to interactions of nanocrystallites with oxygen and another elements or impurities in ambient air. This can dramatically enhance the role of oxidation in formation of PL centers and, in particular, the relative contribution of oxygen-related PL mecha-

Downloaded 25 Feb 2002 to 132.204.56.48. Redistribution subject to AIP license or copyright, see http://ojps.aip.org/japo/japcr.jsp

nisms. Indeed, we recorded a considerable enhancement of 1.6–1.7 eV signals and appearance of additional 2.2–2.3 eV signals under prolonged natural oxidations of highly porous films in air [Figs. 7(a) and 7(b)]. Strong oxidation caused by a thermal annealing of the films also led to the generation of 2.2–2.3 eV signals. Here, one may add that a direct pulsed laser ablation of silicon in pure oxygen resulted in similar 2.2–2.3 eV signals.[20] It should be noted that similar components were observed in many previous studies with the use of various fabrication techniques (see, e.g., Refs. 3, 4, and 21–25). The origin of 2.2–2.3 eV PL seems to be relatively clear since it was thoroughly examined in some previous studies of highly oxidized porous silicon[3] and various Si-based films (see, e.g., Refs. 22, 24, and 25). This component was unambiguously attributed to a radiative recombination through defects in $SiO_2$ structure such as the nonbridging oxygen hole centers.[3,26] The defects are formed in oxygen-related silicon compounds, in particular under the thermal annealing[3] or a prolonged film exposition to air.[24] In our experiments, the 2.2–2.3 eV component was also recorded after the thermal annealing in air, a prolonged humid oxidation of some films deposited in helium, and direct deposition of silicon in pure oxygen.[20] We suppose that the 2.2–2.3 eV PL centers are effectively formed under a strong oxidation of Si-based films, which was the common feature of these cases. The supposition is confirmed by the results of a chemical attack of the films by HF solutions, which led to a compete disappearance of 2.2–2.3 eV signals due to a removal of the thick oxide shell.

A gradual growth of the integral intensity of 1.6–1.7 eV signals, with the time of the film prolonged exposition to air, also gives an evidence for a contribution of oxygen in a formation of the PL signals. Similar phenomenon was recorded on films, deposited in an oxygen-free atmosphere by a laser decomposition of silane.[2,4] However, there is no consensus on the origin of these signals in the literature. Taking account of the size-independent behavior of the 1.6–1.7 eV signals, some authors attribute it to a recombination through an interfacial layer between the c-Si core and the a-$SiO_2$ surface layer.[2] Our results on the chemical attack of the films are also not in contradiction with this mechanism. Indeed, the 1.6–1.7 eV signals appeared every time after the attack as soon as the surface natural oxidation led to a recovery of the interfacial layer. On the other hand, some properties of the red components such as a relatively long decay, enable to ascribe it to the quantum confinement mechanism (see, e.g., Refs. 22, 23, and 25). In this case, the increase of the PL efficiency during the prolonged natural oxidation could be explained by a better dangling bond passivation.

It is clear that in normal conditions, oxidation-related mechanisms give the strongest contribution when integral surface area of the film is maximal, but the pores give however enough access to the inner film layers for oxygen and other elements. This compromise was probably achieved under 65%–80% porosity, which led to the most efficient modification of PL characteristics with storage time in air and the strongest signals of 1.6–1.7 eV and 2.2–2.3 eV components.

Finally, we can not exclude that the mentioned discrepancy of experimental results related to the presence[8,9] or absence[2,4–7] of size dependence for PL spectra were because of different film microstructures in different studies. Relatively porous films could provide better conditions for oxidation-related mechanisms, while low porous films contributed to the preferential contribution of another mechanisms, e.g., the quantum confinement one. In any case, our studies show that the film morphology must be taken into account in the interpretation of experimental results to avoid possible ambiguities and misunderstandings.

## VI. CONCLUSIONS

$Si/SiO_x$ nanostructured films exhibiting visible PL have been fabricated by a pulsed laser ablation in helium residual gas. It has been established that not only the mean particle size, but also the microstructure of the films, are extremely sensitive to deposition conditions. Depositions under different helium pressures can lead to quite different porosities of the laser-ablated films.

It has been also found that porous microstructure can strongly effect the PL properties of the laser-ablated films. The low-porous film structure minimizes the effect of postdeposition natural oxidation on PL properties. In this case, PL signals with peak energies between 1.6 and 2.15 eV depending on helium pressure during the deposition are observed. In contrast, PL properties of highly porous films are mainly determined by postdeposition oxidation phenomena. They lead to an appearance and enhancement of PL bands around 1.6–1.7 eV and 2.2–2.3 eV, which are independent of the deposition conditions.

## ACKNOWLEDGMENTS

The authors are grateful to Professor Richard Leonelli for assistance during PL measurements, Suzie Poulin for XPS measurements, and to Jean-Paul Levesque for technical assistance.

[1] L. T. Canham, Appl. Phys. Lett. **57**, 1046 (1990).
[2] Y. Kanemitsu, T. Ogawa, K. Shiraishi, and K. Takeda, Phys. Rev. B **48**, 4883 (1993).
[3] S. M. Prokes, Appl. Phys. Lett. **62**, 3244 (1993).
[4] S. Botti, R. Coppola, F. Gourbilleau, and R. Rizk, J. Appl. Phys. **88**, 3396 (2000).
[5] Y. Yamada, T. Orii, I. Umezu, S. Takeyama, and T. Yoshida, Jpn. J. Appl. Phys., Part 1 **35**, 1361 (1996).
[6] T. Makimura, Y. Kunii, and K. Murakami, Jpn. J. Appl. Phys., Part 1 **35**, 4780 (1996).
[7] I. Umezu, K. Shibata, S. Yamaguchi, A. Sugimura, Y. Yamada, and T. Yoshida, J. Appl. Phys. **84**, 6448 (1998).
[8] M. Ehbrecht, B. Kohn, F. Huisken, M. A. Laguna, and V. Paillard, Phys. Rev. B **56**, 6958 (1997).
[9] L. Patrone, D. Nelson, V. I. Safarov, M. Sentis, W. Marine, and S. Giorgio, J. Appl. Phys. **87**, 3829 (2000).
[10] A. V. Kabashin, M. Charbonneau-Lefort, M. Meunier, and R. Leonelli, Appl. Surf. Sci. **168**, 328 (2000).
[11] L. A. Chiu, A. A. Seraphin, and K. D. Kolenbrander, J. Electron. Mater. **23**, 347 (1994).
[12] I. A. Movtchan, W. Marine, R. W. Dreyfus, U. C. Lee, M. Sentis, and M. Autric, Appl. Surf. Sci. **96**, 251 (1996).
[13] D. B. Geohegan, A. A. Puretzky, G. Duscher, and S. J. Pennycook, Appl. Phys. Lett. **72**, 2987 (1998).
[14] L. T. Paratt, Phys. Rev. **95**, 359 (1954).

Downloaded 25 Feb 2002 to 132.204.56.48. Redistribution subject to AIP license or copyright, see http://ojps.aip.org/japo/japcr.jsp

[15] D. H. Lowndes, C. M. Rouleau, T. Thundat, G. Duscher, E. A. Kenik, and S. J. Pennycook, Appl. Surf. Sci. **127**, 355 (1998).
[16] E. Chason and T. M. Mayer, Crit. Rev. Solid State Mater. Sci. **22**, 1 (1997).
[17] V. Holy, U. Pietsch, and T. Baumbach, Springer Tracts Mod. Phys. **149**, 5 (1999).
[18] M. Tolan, Springer Tracts Mod. Phys. **148**, 7 (1999).
[19] S. Hayashi, S. Tanimoto, and K. Yamamoto, J. Appl. Phys. **68**, 5300 (1990).
[20] A. V. Kabashin, M. Meunier, and R. Leonelli, J. Vac. Sci. Technol. B **19**, 2217 (2001).
[21] E. Edelberg, S. Bergh, R. Naone, M. Hall, and B. S. Aydil, Appl. Phys. Lett. **68**, 1415 (1996).
[22] K. S. Min, K. V. Shcheglov, C. M. Yang, H. A. Atwater, M. L. Brongersma, and A. Polman, Appl. Phys. Lett. **69**, 2033 (1996).
[23] S. Li, S. J. Silvers, and M. S. El-Shall, J. Phys. Chem. B **101**, 1794 (1997).
[24] H. Tamura, M. Ruckschloss, T. Wirschem, and S. Veptek, Appl. Phys. Lett. **65**, 1537 (1994).
[25] A. J. Kenyon, P. F. Trwoga, C. W. Pitt, and G. Rehm, J. Appl. Phys. **79**, 9291 (1996).
[26] S. Munekuni, T. Yamanaka, Y. Shimogaichi, K. Nagasawa, and Y. Hama, J. Appl. Phys. **68**, 1212 (1990).

**Downloaded 25 Feb 2002 to 132.204.56.48. Redistribution subject to AIP license or copyright, see http://ojps.aip.org/japo/japcr.jsp**